

Periodic laminar forced convection: solution via symbolic computation and integral transforms

Silvia Cheroto^a, Mikhail Dimitrov Mikhailov^b, Sadik Kakaç^a, Renato Machado Cotta^{b*}

^a Mechanical Engineering Department, University of Miami, P.O. Box 248294, Coral Gables, FL, 33124-0624, USA

^b Laboratory of Transmission & Technology of Heat, LTTC – DEM/EE & PEM/COPPE, Universidade Federal do Rio de Janeiro, C.P. 68503, Rio de Janeiro, RJ, 21945-970, Brazil

(Received 2 June 1998, accepted 7 January 1999)

Abstract — Transient laminar forced convection within the thermal entrance region of parallel-plate channels is analytically solved for by making use of the Generalized Integral Transform Technique (GITT) and mixed symbolic-numerical computation (*Mathematica* 3.0 system). The physical situation involves a periodic variation in time of the fluid inlet temperature, together with a fifth kind boundary condition at the channel walls that includes external convection and wall thermal capacitance effects. A mixed symbolic-numeric algorithm is constructed, which provides fully automatic derivation of all the analytical steps and offers a straightforward visualization of the numerical results, in both tabular and graphical forms. Amplitudes and phase lags of the system thermal response are then presented and interpreted, while critically compared with previously reported results. © Elsevier, Paris.

periodic convection / integral transforms / symbolic computation / cooling of electronics / hybrid methods

Résumé — Convection forcée laminaire périodique : solution utilisant le calcul symbolique et les transformées intégrales. La convection forcée laminaire transitoire à l'entrée thermique d'un canal formé par deux plans parallèles est résolue analytiquement au moyen de la technique de la transformée intégrale généralisée (GITT), en utilisant un mélange de calcul symbolique et numérique (à l'aide du logiciel *Mathematica* 3.0). Les conditions imposées correspondent, d'une part, à une variation périodique de la température du fluide à l'entrée et, d'autre part, à une condition limite à la paroi du canal, qui inclut la convection externe et les effets dus à la capacité thermique des parois. Un algorithme mêlant calcul symbolique et numérique est construit. Il permet d'obtenir automatiquement les résultats numériques sous forme tabulée ou graphique. Les amplitudes et les déphasages de la réponse thermique du système sont représentées et interprétées. © Elsevier, Paris.

convection périodique / transformées intégrales / calcul symbolique / refroidissement de composants électroniques / méthodes hybrides

Nomenclature

a^*	fluid-to-wall thermal capacitance ratio ($= \rho c_p)_f d / (\rho c)_w L$)	h_e	equivalent heat transfer coefficient between inner wall and ambient fluid
Bi	equivalent Biot number ($= h_e d / k_f$)	i	imaginary number $\sqrt{-1}$
c	wall specific heat $\text{kJ}\cdot\text{kg}^{-1}\cdot\text{K}^{-1}$	k_f	fluid thermal conductivity $\text{W}\cdot\text{m}^{-1}\cdot\text{K}^{-1}$
c_p	fluid specific heat $\text{kJ}\cdot\text{kg}^{-1}\cdot\text{K}^{-1}$	L	wall thickness m
d	half distance between the parallel plated m	\dot{m}	mass flow rate $\text{kg}\cdot\text{s}^{-1}$
D_e	equivalent diameter of the channel m	N	normalization integral or truncation order of the system
		Pr	Prandtl number ($= \nu / \alpha$)
		Re	Reynolds number ($= (U_m D_h / \nu)$)
		T	temperature K or °C

* cotta@serv.com.ufrj.br



$T(x, y, t)$	temperature distribution along the channel K or °C	
T_∞	ambient temperature K or °C	
T_{c0}	centerline inlet temperature K or °C	
$\Delta T(y)$	inlet temperature amplitude profile	
ΔT_c	centerline inlet temperature amplitude ($= T_{c0} - T_\infty$)	
t	time variable	s
$u(y)$	velocity profile across the plates	$\text{m}\cdot\text{s}^{-1}$
U_m	mean velocity	$\text{m}\cdot\text{s}^{-1}$
$U(\eta)$	dimensionless velocity profile ($= u(y)/U_m$)	
x	axial coordinate	m
y	normal coordinate	m

Greek symbols

α	fluid thermal diffusivity ($= (k_f/\rho c_p)$)	$\text{m}^2\cdot\text{s}^{-1}$
β	inlet frequency	Hz
$\Delta\Theta(\eta)$	dimensionless temperature amplitude profile across the inlet	
δ_{ij}	function; for $i = j$, $\delta = 1$; for $i \neq j$, $\delta = 0$ (ij or any other indexes)	
Φ	phase lag	
η	dimensionless normal coordinate ($= y/d$)	
λ	eigenvalue	
ν	kinematic viscosity of the fluid	$\text{m}^2\cdot\text{s}^{-1}$
$\Theta(\xi, \eta, \tau)$	dimensionless temperature	
$\bar{\Theta}(\xi, \eta)$	quasi-steady dimensionless temperature defined by equation (4)	
ρ	density of the working fluid	$\text{kg}\cdot\text{m}^{-3}$
ρ_w	equivalent density of the wall	$\text{kg}\cdot\text{m}^{-3}$
μ	viscosity	$\text{N}\cdot\text{s}\cdot\text{m}^{-2}$
τ	dimensionless time ($= \alpha t/d^2$)	
Ω	dimensionless inlet frequency ($= d^2 \beta/\alpha$)	
ξ	dimensionless axial coordinate ($= (x/D_e) (D_e/d)^2/Re Pr$)	

Subscripts

c	centerline value
f	working fluid value
n, k	order of the eigenvalue problem
w	wall value
∞	ambient value or value at infinite

1. INTRODUCTION

Unsteady forced convection is an important topic in the field of heat transfer technology, in relation with the automatic control of heat exchange equipment.

Unsteady problems, with respect to their dependence with time, may be classified as transient or periodic. Clearly, the steady part of the solution of a periodic problem should be simpler than its transient (or complete) solution, which is often very involved. Yet, in many practical applications, such as the flow and heat transfer associated with vibrating components, some types of engines, heat exchangers, gas turbines and so on, the steady part of the periodic solution is most important. Previous research work on periodic forced convection inside ducts have focused on the development of solution methodologies for the governing flow and energy equations [1–8], with a clear preference for analytic-based approaches, in light of the difficulties in numerically handling high frequency oscillating thermal system responses.

Unsteady heat transfer for fully developed laminar flow inside the thermal entrance region of a parallel plate channel, with a fully developed parabolic velocity profile and subjected to a sinusoidally varying inlet temperature, is considered here. A general boundary condition of the fifth kind, that accounts for the effects of both external convection and wall thermal capacitance, is imposed at the channel walls. This particular problem was also studied by Kakaç et al. [7] and Cheroto et al. [8], and in both contributions the problem was solved by using the generalized integral transform technique (GITT) [9–11], but using different approaches to the same hybrid numerical-analytical solution methodology.

Kakaç et al. [7] studied theoretically and experimentally a laminar forced convection problem in the thermal entrance region of a rectangular duct, subjected to a sinusoidally varying inlet temperature and a fifth kind boundary condition at the walls. The theoretical analysis was performed by using the GITT, instead of attempting a formal exact solution, in order to alleviate the need for solving a complex non classical Sturm-Liouville problem, for which a direct solution was not yet available. Also, experiments were performed in an apparatus previously designed and built by Kakaç et al. [6–7]. The theoretical results were then compared with the experimental findings to verify the approach, with excellent overall agreement.

In Cheroto et al. [8] the same problem [7] was studied by the GITT, but in this latter work, an alternative formulation was developed, in which the problem was divided into real and imaginary formulations, and the analysis was performed by using these two coupled similar problems.

In the present work the method of solution is still the GITT [9–11], but now made more flexible with the choice of a simpler auxiliary eigenvalue problem. Another difference and the main original aspect of this study is, in fact, the special feature of a symbolic computation implementation, such as recently achieved for the simpler slug flow situation [12], by employing the *Mathematica 3.0* system [13], used to handle all the analytical steps of the problem solution procedure, including all the integral transformations and

operational manipulations. The use of the *Mathematica* system [13] for solving heat transfer problems is a new and growing tendency since it has many advantages in dealing with hybrid methods, such as the proposed integral transform method. The main advantages in the use of hybrid symbolic-numerical computational platforms are the drastic reduction in analytical development effort and the straightforward integrated manipulation of data, analytical expressions, and numerical algorithms, including simple to use graphical visualization tools, which in combination lead to a much faster path to the interpretation of the final results. For a complete description of symbolic-numerical computations in the heat transfer field with integral transforms and *Mathematica*, the reader is referred to [11, 14].

2. PROBLEM FORMULATION

We consider unsteady forced convection with hydrodynamic fully developed laminar flow inside the thermal entrance region of a parallel plate channel, subjected to a periodic variation of the inlet temperature, as represented in *figure 1*. A general boundary condition of the fifth kind that accounts for both external convection and wall heat capacitance effects is considered. Axial conduction along the fluid, viscous dissipation and free convection are not taken into consideration and physical properties are assumed to be constant. The problem can be represented by the energy equation and related boundary and inlet conditions as:

$$\frac{\partial T}{\partial t} + u(y) \frac{\partial T}{\partial x} = \alpha \frac{\partial^2 T}{\partial y^2} \quad \text{if } 0 < y < d, x > 0, t > 0 \quad (1a)$$

$$T = T_\infty + \Delta T(y) e^{i\beta t} \quad \text{if } x = 0, 0 < y < d \quad (1b)$$

$$\frac{\partial T}{\partial y} = 0 \quad \text{if } y = 0, x > 0 \quad (1c)$$

$$h_e(T - T_\infty) + k_f \frac{\partial T}{\partial y} + (\rho c)_w L \frac{\partial T}{\partial t} = 0 \quad \text{if } y = d, x > 0 \quad (1d)$$

where the variables are in dimensional form and $T \equiv T(x, y, t)$.

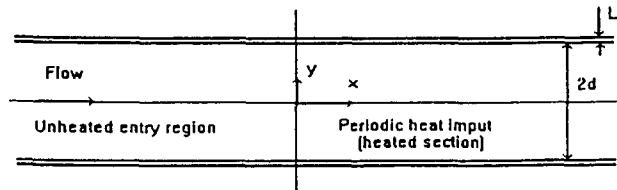


Figure 1. Geometry and coordinate system for theoretical analysis.

Equation (1d) represents the fifth kind boundary condition. The first term is the convection term between the walls and the surrounding fluid (air), at ambient temperature T_∞ , with h_e being the equivalent heat transfer coefficient, which may also account for the transversal thermal resistance of the channel walls. The last term represents the wall thermal capacitance effect. Details on the derivation and calculation of the appropriate values of h_e are given in [15].

The problem is now rewritten in dimensionless form by using the following dimensionless groups:

$$\begin{aligned} \eta &= \frac{y}{d} & \Omega &= \frac{\beta d^2}{\alpha} \\ \xi &= (x/D_e) (D_e/d)^2 / (Re Pr) & a^* &= \frac{(\rho c_p)_f d}{(\rho c)_w L} \\ \tau &= \frac{\alpha t}{d^2} & U(\eta) &= \frac{u(y)}{U_m} \\ \Theta &= \frac{T - T_\infty}{\Delta T_c} & \Delta\Theta(\eta) &= \frac{\Delta T(y)}{\Delta T_c} \\ Bi &= \frac{h_e d}{j_f} \end{aligned} \quad (2a-i)$$

where $\Theta \equiv \Theta(\xi, \eta, \tau)$.

By making use of the dimensionless groups given by equations (2) in the energy equation and the related boundary conditions, equations (1a-d), the problem can be written in dimensionless form as:

$$\frac{\partial \Theta}{\partial \tau} + U(\eta) \frac{\partial \Theta}{\partial \xi} = \frac{\partial^2 \Theta}{\partial \eta^2} \quad \text{if } 0 < \eta < 1, \xi > 0 \quad (3a)$$

$$\Theta = \Delta\Theta(\eta) e^{i\Omega\tau} \quad \text{if } \xi = 0, 0 \leq \eta \leq 1 \quad (3b)$$

$$\frac{\partial \Theta}{\partial \eta} = 0 \quad \text{if } \eta = 0, \xi > 0 \quad (3c)$$

$$Bi \Theta + \frac{\partial \Theta}{\partial \eta} + \frac{1}{a^*} \frac{\partial \Theta}{\partial \tau} = 0 \quad \text{if } \eta = 1, \xi > 0 \quad (3d)$$

Note that if a^* , the fluid-to-wall thermal capacitance ratio, goes to infinity, the wall capacitance effects become negligible.

3. PERIODIC SOLUTION

We are only interested in the periodic solution of the problem, for sufficiently large values of the time variable, i.e. after the initial transients have disappeared. For such cases, a periodic solution can be assumed as:

$$\Theta(\xi, \eta, \tau) = e^{i\Omega\tau} \bar{\Theta}(\xi, \eta) \quad (4)$$

for the decay of the inlet condition, equation (3b), within the duct. Upon substitution of the periodic solution,

equation (4), the problem given by equations (3) simplifies to the following problem for $\bar{\Theta}(\xi, \eta)$:

$$\frac{\partial^2 \bar{\Theta}}{\partial \eta^2} - U(\eta) \frac{\partial \bar{\Theta}}{\partial \xi} - i \Omega \bar{\Theta} = 0 \text{ if } 0 < \eta < 1, \xi > 0 \quad (5a)$$

$$\bar{\Theta} = \Delta \bar{\Theta}(\eta) \text{ if } \xi = 0, 0 \leq \eta \leq 1 \quad (5b)$$

$$\frac{\partial \bar{\Theta}}{\partial \eta} = 0 \text{ if } \eta = 0 \quad (5c)$$

$$Bi \bar{\Theta} + \frac{\partial \bar{\Theta}}{\partial \eta} + \frac{1}{a^*} i \Omega \bar{\Theta} = 0 \text{ if } \eta = 1 \quad (5d)$$

4. SOLUTION METHODOLOGY (GITT)

The approach used here is the generalized integral transform technique (GITT) [9–11]. The use of the GITT allows for the selection of an appropriate auxiliary eigenvalue problem, without being restricted to the specific problem that would allow for a transformable solution. A formal exact solution for this problem is achieved by considering the associated complex eigenvalue problem, that includes both complex terms in the original equation and in the boundary condition. However, its solution is a complicated matter by itself. In [7, 8], the eigenvalue problem was chosen as the same that provides the exact solution of the classical Graetz problem, defined in the real domain, with good performance as a basis of the proposed expansion. Here, an even simpler eigenvalue problem is considered, since all the required manipulations are automatically worked out by the symbolic computation system:

$$\frac{d^2 \tilde{Y}_n}{d\eta^2} + \lambda_n^2 \tilde{Y}_n = 0 \text{ if } 0 < \eta < 1 \quad (6a)$$

$$\frac{d\tilde{Y}_n}{d\eta} = 0 \text{ if } \eta = 0 \quad (6b)$$

$$Bi \tilde{Y}_n + \frac{d\tilde{Y}_n}{d\eta} = 0 \text{ if } \eta = 1 \quad (6c)$$

for $\tilde{Y}_n \equiv \tilde{Y}_n(\eta)$, and where \tilde{Y}_n 's and λ_n 's are the n -th normalized eigenfunction and eigenvalue, respectively, and the normalization is defined as

$$\tilde{Y}_n(\eta) = \frac{Y_n(\eta)}{\sqrt{N_n}} \quad (6d)$$

The normalization integral is given by:

$$N_n = \int_0^1 \tilde{Y}_n^2(\eta) \, d\eta \quad (6e)$$

The solution for the eigenvalue problem (6a-c) is given by:

$$\tilde{Y}_n(\eta) = \cos(\lambda_n \eta) \quad (6f)$$

where the eigenvalues are obtained from the nonlinear equation

$$-\lambda_n \sin \lambda_n + Bi \cos \lambda_n = 0 \quad (6g)$$

By solving the transcendental equation (6g) above we can readily find the λ_n 's.

The auxiliary eigenvalue problem allows the definition of the integral transform pair (inversion and transform formula) for the function $\bar{\Theta}(\xi, \eta)$, given by:

$$\bar{\Theta}(\xi, \eta) = \sum_{n=1}^{\infty} \tilde{Y}_n(\eta) \bar{\Theta}_n(\xi) \text{ if } 0 < \eta < 1 \quad (inversion formula) \quad (7a)$$

and

$$\bar{\Theta}_n(\xi) = \int_0^1 \tilde{Y}_n(\eta) \bar{\Theta}(\xi, \eta) \, d\eta \quad (transform formula) \quad (7b)$$

By making use of the integral transform pair and operating on equations (5a-d) and (6a-c), the periodic problem and the eigenvalue problem respectively, the integral transformation can be formulated, to get the transformed equation as:

$$\frac{i \Omega}{a^*} \tilde{Y}_n(1) \sum_{k=1}^{\infty} \tilde{Y}_k(1) \bar{\Theta}_k(\xi) - \lambda_n^2 \bar{\Theta}_n(\xi) - \sum_{k=1}^{\infty} \frac{d\bar{\Theta}_k(\xi)}{d\xi} Q_{nk} - i \Omega \bar{\Theta}_n(\xi) = 0 \quad (8)$$

Note that the integral transformation eliminated the problem dependence in η . Now we can rewrite equation (8) in matrix form as:

$$Q \frac{d\bar{\Theta}}{d\xi} = B \bar{\Theta} \quad (9a)$$

where

$$Q = \{Q_{nk}\} \quad (9b)$$

and

$$B = \{B_{nk}\} \quad (9c)$$

with

$$Q_{nk} = \int_0^1 \tilde{Y}_n(\eta) U(\eta) \tilde{Y}_k(\eta) \, d\eta \quad (9d)$$

$$B_{nk} = -(\lambda_k^2 + i \Omega) \delta_{nk} - \frac{i \Omega}{a^*} \tilde{Y}_k(1) \tilde{Y}_n(1) \quad (9e)$$

where δ represents the Kroneker delta. Rearranging,

$$\frac{d\bar{\theta}}{d\xi} = A \bar{\theta} \tag{9f}$$

where

$$A = Q^{-1} B \tag{9g}$$

We need now to transform the inlet condition by operating on equation (5b) with $\int_0^1 \tilde{Y}_n(\eta) d\eta$, to obtain:

$$\bar{\theta}_n(0) = f_n(\eta) \tag{10a}$$

with

$$f_n(\eta) = \int_0^1 \tilde{Y}_n(\eta) \Delta\theta(\eta) d\eta \tag{10b}$$

Finally, the transformed system is defined by equations (9f, 10a), and this linear initial value problem can be analytically handled by obtaining the related complex eigenvalues and eigenvectors of the complex coefficients matrix **A**. The inversion formula (7b) is then recalled to reconstruct the desired potentials.

5. SYMBOLIC COMPUTATION

All the above and intermediate manipulations are automatically accomplished by the symbolic implementation on the *Mathematica* system. The symbolic computations were performed by adapting one of the notebooks available in [11], where the eigenvalues, eigenvectors, normalization integrals, the coefficients matrix **A**, and all the remaining terms are calculated by *Mathematica 3.0* in order to generate $\text{Abs}[\theta[\xi,\eta]]$, which represents the amplitude of the temperature distribution θ , and $\text{Arg}[\theta[\xi,\eta]]$, which represents the phase angle (phase lag) of the temperature distribution θ . The 3D plots are easily generated as outputs and in each of them the amplitudes and phase angles are represented. In these plots, the vertical distances represent the amplitudes. The phase angles are represented by the color variation along the 3D surface, not visualized in the presentation that follows (which is shown in a gray scale), but readily reproducible from the notebook presented in the Appendix. As the angle moves around the circle, the color of the surface will go from red to blue, green, yellow, and back to red again. Therefore the plots provide all information about the temperature oscillations required for its physical interpretation.

A copy of the *Mathematica* notebook used here in order to get the final results for amplitudes and phase lags is presented in the Appendix.

6. RESULTS AND DISCUSSIONS

Initially, convergence tests and comparisons were performed to verify the reliability of the present results. The first two tables present the convergence behavior of the centerline temperature amplitude for two different cases of Biot number, $Bi = 10$ and 10^5 , respectively (*tables I and II*). The dimensionless temperature amplitude profile across the inlet, $\Delta\theta(\eta)$, was taken as parabolic, approximating the actual physical situation encountered in refs. [7, 8]. For the case of large Biot number (*table I*), the convergence is very fast and the results are fully converged with six terms in the expansion ($N = 6$), up to the fourth significant digit. The positions ξ were chosen mostly in the beginning of the duct, where the convergence behavior is expected to be worse.

TABLE I
Convergence of the centerline temperature amplitude for $Bi = 10^5$, $\Omega = 0.06491$, $a^* = 5.0 \cdot 10^{-5}$, and $\Delta\theta(\eta) = 1 - \eta^2$.

ξ	0.01	0.1	0.5	1.0
$N = 3$	0.9864	0.8561	0.4055	0.1580
$N = 6$	0.9866	0.8562	0.4056	0.1580
$N = 9$	0.9866	0.8562	0.4056	0.1580
$N = 12$	0.9866	0.8562	0.4056	0.1580

TABLE II
Convergence of the centerline temperature amplitude for $Bi = 10$, $\Omega = 0.06491$, $a^* = 5.0 \cdot 10^{-5}$, and $\Delta\theta(\eta) = 1 - \eta^2$.

ξ	0.01	0.1	0.5	1.0
$N = 3$	0.9112	0.8175	0.3232	0.0999
$N = 6$	0.9943	0.8578	0.3806	0.1363
$N = 9$	0.9835	0.8520	0.3886	0.1441
$N = 12$	0.9881	0.8559	0.3948	0.1486
$N = 15$	0.9856	0.8544	0.3966	0.1505
$N = 18$	0.9872	0.8558	0.3988	0.1521
$N = 21$	0.9861	0.8551	0.3995	0.1529

For smaller values of the Biot number the convergence behavior became worse, which is an indication that a filter should be employed for convergence improvement, if necessary. This behavior is due to the presence of the source term represented by the wall thermal capacitance term, which is not accounted for by the eigenvalue problem boundary condition. For larger Biot numbers, this effect loses importance with respect to the external convection term. For this case

($Bi = 10$), the results with $N = 21$ in *table II* are converged to ± 1 in the third significant digit, which is more than sufficient for the physical interpretation of the thermal response of the system.

In order to validate the present approach, comparisons were made between the present work and two previous ones. First, for the case when the Biot number tends to infinity, but now with a linear inlet profile ($\Delta\theta(\eta) = 1$), the results were compared with the results of reference [8], as presented in *table III*.

TABLE III
Comparison between the present work and reference [8] for the convergence of the centerline temperature amplitude with $Bi = 10^5$, $\Omega = 0.06491$, $a^* = 5.0 \cdot 10^{-5}$, and $\Delta\theta(\eta) = 1$

x/D_e	$N = 5$	$N = 10$	Ref. [8], $N_c = 5$
1	0.9990	0.9990	0.9990
3	0.9282	0.9278	0.9277
6	0.7475	0.7472	0.7471
9	0.5912	0.5909	0.5908
12	0.4668	0.4666	0.4665
15	0.3685	0.3684	0.3683
18	0.2910	0.2908	0.2908
21	0.2297	0.2296	0.2296
24	0.1814	0.1813	0.1813
27	0.1432	0.1431	0.1431
30	0.1130	0.1130	0.1130
33	0.0892	0.0892	0.0892
36	0.0705	0.0704	0.0704
39	0.0556	0.0556	0.0556

the results of the present work and ref. [7] were too small to be noticeable in graphical form. The number of terms $N = 15$ was the maximum shown in *table IV*, but was already enough to offer 2 to 3 significant digits accuracy along the whole thermal entry region. Again, a filtering solution, as generally employed in solutions through the integral transform approach [9–11], can considerably enhance this convergence behavior, although it was not found necessary for the objectives of the present work.

TABLE IV
Comparison between the present work and reference [7] for the convergence of the centerline temperature amplitude with $Bi = 10$, $\Omega = 0.06491$, $a^* = 5.0 \cdot 10^{-5}$, and $\Delta\theta(\eta) = 1$

x/D_e	$N = 6$	$N = 9$	$N = 12$	$N = 15$	Ref. [7], $N_c = 60$
1	1.0076	1.0008	1.0008	0.9977	0.9990
3	0.9216	0.9187	0.9244	0.9235	0.9222
6	0.7250	0.7301	0.7375	0.7385	0.7341
9	0.5612	0.5702	0.5781	0.5801	0.5743
12	0.4339	0.4447	0.4526	0.4550	0.4486
15	0.3354	0.3468	0.3542	0.3569	0.3504
18	0.2593	0.2705	0.2773	0.2799	0.2737
21	0.2004	0.2109	0.2170	0.2195	0.2138
24	0.1549	0.1645	0.1699	0.1722	0.1670
27	0.1196	0.1283	0.1330	0.1350	0.1304
30	0.0925	0.1000	0.1041	0.1059	0.1019
33	0.0716	0.0780	0.0815	0.0831	0.0796
36	0.0553	0.0608	0.0638	0.0652	0.0622
39	0.0428	0.0474	0.0511	0.0511	0.0485

The dimensionless position x/D_e is employed in the comparisons with the results from reference [8]. N_c is the number of terms used in the expansion proposed in reference [26], with a different eigenvalue problem. The convergence for three significant digits is attained for $N \leq 10$ terms, and it is harder to achieve in the channel entrance, as expected. The comparison shows an excellent agreement between the two sets of results.

In order to investigate more critically the accuracy of the present results, a more difficult case in terms of convergence is analyzed, for $Bi = 10$. This comparison was made between the present work and the work by Kakaç et al. [7], with the reference results presented in the last column, converged for $N_c = 60$ terms, where N_c denotes the number of terms from the expansion proposed in [7]. This comparison is presented in *table IV* below, and clearly shows that convergence slows down considerably in this case, but the differences between

Now that the code is shown to be reliable for our present purposes, a series of 3D plots are presented, where the temperature amplitude and the phase angle are computed and shown. In these plots, the vertical distances represent the amplitudes. The phase angles are represented by the color variation along the 3D surface. As the angle moves around the circle, the color of the surface will go from red to blue, green, yellow, and back to red again. This effect is observed here on a gray scale only, but is readily observable when employing the *Mathematica* notebook. The test cases selected have the following additional parameters: $Bi = 10$, $a^* = 8.5 \cdot 10^{-3}$, and the inlet temperature profile is a parabolic one represented by $\Delta\theta(\eta) = 1 - \eta^2$. The plots are for $0 \leq \eta \leq 1$, from the center of the channel to the wall, and $0 \leq \xi \leq 5$, where the value 5 represents a very large distance from the inlet, where the flow is essentially fully developed.

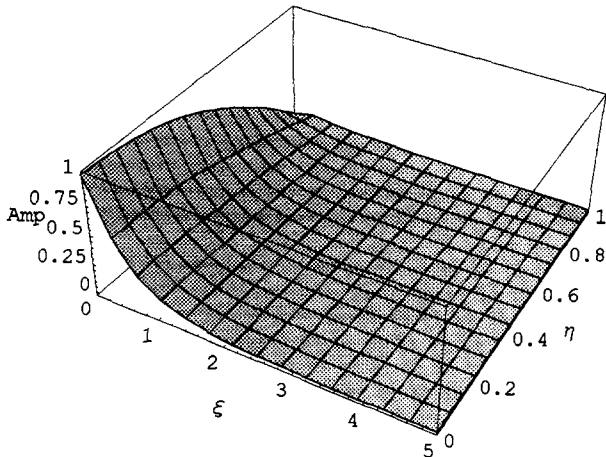


Figure 2. Temperature amplitude and phase lag. $Bi = 10$, $\Omega = 0.06491$, $a^* = 8.5 \cdot 10^{-3}$ and $\Delta\theta(\eta) = 1 - \eta^2$.

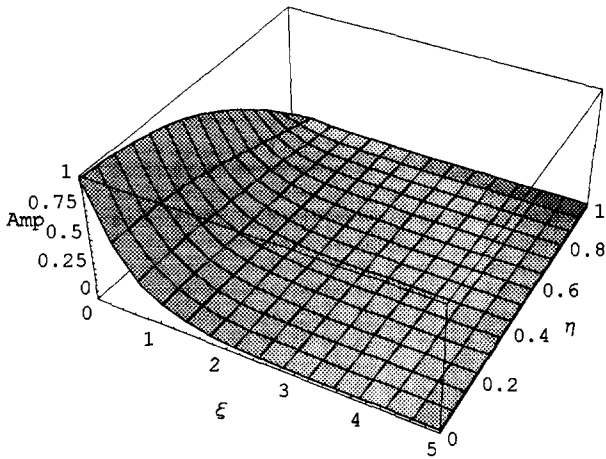


Figure 3. Temperature amplitude and phase lag. $Bi = 10$, $\Omega = 0.13220$, $a^* = 8.5 \cdot 10^{-3}$ and $\Delta\theta(\eta) = 1 - \eta^2$.

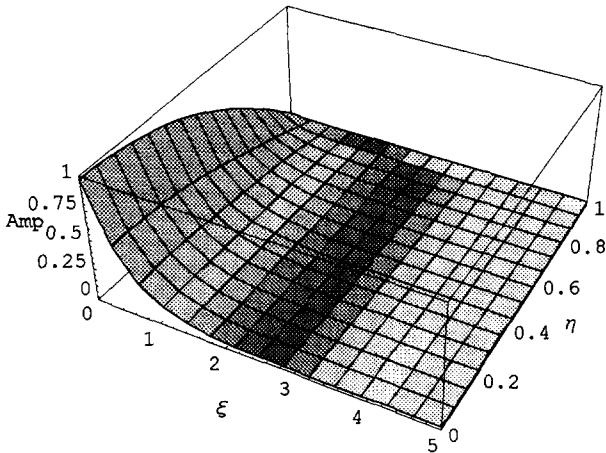


Figure 4. Temperature amplitude and phase lag. $Bi = 10$, $\Omega = 1.0$, $a^* = 8.5 \cdot 10^{-3}$ and $\Delta\theta(\eta) = 1 - \eta^2$.

The varying parameter is the dimensionless inlet frequency Ω , with $\Omega = 0.06491$, $\Omega = 0.13220$, and $\Omega = 1.0$, respectively in figures 2, 3, and 4. As can be noticed, the amplitude does not noticeably vary with Ω , only the phase angle. For a larger value of Ω , $\Omega = 1$, the change in the phase angle can be clearly observed. As Ω increases, the change in the phase angle increases, thus further delaying the information sensed along the channel with respect to the inlet condition oscillation. All the results in the plots were obtained with $N = 20$.

7. CONCLUDING REMARKS

The procedure here developed was shown to be efficient in the solution of thermally developing periodic forced convection. A filtering approach can be considered and implemented in order to alleviate convergence difficulties. The symbolic computation feature proposed through the *Mathematica 3.0* system is a new tendency and proved to be simple to use and also powerful in the solution of this class of problems. The graphics representation is easy to implement and markedly facilitates the physical analysis task.

Acknowledgment

The authors would like to acknowledge the financial support provided by CNPq/Brazil and NSF/USA, in the scope of this international cooperation project.

REFERENCES

- [1] Sparrow E.M., de Farias F.N., Unsteady heat transfer in ducts with time varying inlet temperature and participating walls, *Int. J. Heat Mass Tran.* 11 (5) (1968) 837-853.
- [2] Kakaç S., Yener Y., Exact solution of the transient forced convection energy equation for timewise variation of inlet temperature, *Int. J. Heat Mass Tran.* 16 (2) (1973) 2205-2214.
- [3] Kakaç S., A general analytical solution to the equation of transient forced convection with fully developed flow, *Int. J. Heat Mass Tran.* 18 (12) (1975) 1449-1453.
- [4] Cotta R.M., Özisik M.N., Laminar forced convection inside ducts with periodic variation of inlet temperature, *Int. J. Heat Mass Tran.* 29 (10) (1986) 1495-1501.
- [5] Cotta R.M., Mikhailov M.D., Özisik M.N., Transient conjugated forced convection in ducts with periodically varying inlet temperature, *Int. J. Heat Mass Tran.* 30 (10) (1987) 2073-2082.
- [6] Kakaç S., Ding Y., Li W., Experimental study of unsteady laminar forced convection in ducts for timewise varying inlet temperature, *Proceeding of the 1st World Conference on Experimental Heat Transfer, Fluid Mechanics and Thermodynamics*, September 4-9, Dubrovnik, Yugoslavia, 1988.
- [7] Kakaç S., Li W., Cotta R.M., Unsteady laminar forced convection in ducts with periodic variation of inlet temperature, *J. Heat Trans.-T. ASME*, 112 (4) (1990) 913-920.

[8] Cheroto S., Santos C.A.C., Kakaç S., Hybrid-analytical investigation of unsteady forced convection in parallel-plate channels for thermally developing flow, *Heat and Mass Transfer, Wärme-und Stoffübertragung*, vol. 32, 1997, pp 317-324.

[9] Cotta R.M., *Integral transforms in computational heat and fluid flow*, CRC Press, Boca Raton, Florida, 1993.

[10] Cotta R.M., Benchmark results in computational heat and fluid flow: the integral transform method, *Int. J. Heat Mass Tran.* 37 (1994) 381-393.

[11] Cotta R.M., Mikhailov M.D., *Heat Conduction: Lumped Analysis, Integral Transforms, Symbolic Computation*, John Wiley & Sons, New York, 1997.

[12] Mikhailov M.D. and Cotta R.M., Temperature oscillations in a slug tube flow, *International Communications in Heat and Mass Transfer* 24 (4) (1997) 575-578.

[13] Wolfram S., *Mathematica: A System for Doing Mathematics by Computer*, 2nd edition, Addison-Wesley, 1991.

[14] Cotta R.M. (Ed.), *The Integral Transform Method in Thermal & Fluids Sciences and Engineering*, Begell House Inc., New York, 1998.

[15] Cheroto S., Analysis of unsteady forced convection in channels by integral transform technique and experiments, Thesis, Mech. Eng. Dept., University of Miami, USA, 1998.

APPENDIX

This appendix presents the Mathematica notebook that was implemented in order to obtain the final results for the periodic forced convection problem studied here. An application example is also presented. External modules were also employed, which are described in more detail in [11, 14].

Statement of the dimensionless problem

The temperature field is governed by:

$$I \Omega \theta[\xi, \eta] + u[\eta] \partial_{\xi} \theta[\xi, \eta] == \partial_{\eta, \eta} \theta[\xi, \eta]$$

The boundary condition at $\eta = 0$ is:

$$\partial_{\eta} \theta[\xi, \eta] == 0 /. \eta \rightarrow 0$$

The boundary condition at $\eta = 1$ is:

$$\partial_{\eta} \theta[\xi, \eta] + Bi \theta[\xi, \eta] + I \frac{\Omega}{as} \theta[\xi, \eta] == 0 /. \eta \rightarrow 1$$

The initial temperature is:

$$\theta[0, \eta] == \theta_0 + \theta_1 \eta + \theta_2 \eta^2$$

Computational rules - GITT

The eigenvalues are computed once and stored in the memory by the rule:

$$\begin{aligned} \mu[i_Integer, Bi_?NumericQ] &:= \mu[i, Bi] \\ &= x /. FindRoot[Bi Cos[x] == x Sin[x], \{x, \{i-1, i-\frac{1}{2}\} \pi\} \\ &\hspace{15em} MaxIterations \rightarrow 30] \end{aligned}$$

The rule for eigenfunction is:

$$\psi[i_Integer][y_]:= c[i, Bi] Cos[\mu[i, Bi]y]$$

where the normalization coefficients $c[i, Bi]$ are computed once and stored in the memory by the rules:

$$c[i_Integer, Bi_?NumericQ] := c[i, Bi] = \frac{(\sqrt{2} Bi Csc[\mu[i, Bi]])}{\sqrt{Bi + Bi^2 + \mu[i, Bi]^2}}$$

The rules for the coupling integral are:

$$\begin{aligned} A[i_-, i_]&:= \frac{1}{8 \mu[i, Bi]^4} (4 \mu[i, Bi]^4 \psi[i][0]^2 \\ &+ 3 Bi \psi[i][1]^2 + 3 \mu[i, Bi]^2 (\psi[i][0]^2 - 2 \psi[i][1]^2)) \\ A[i_-, j_]&:= \frac{3 (2 Bi (1 + Bi) + \mu[i, Bi]^2 + \mu[j, Bi]^2) \psi[i][1] \psi[j][1]}{(\mu[i, Bi]^2 - \mu[j, Bi]^2)^2} \end{aligned}$$

To improve efficiency we introduce the matrices:

$$\begin{aligned} mA &:= Table[A[i, j], \{i, n\}, \{j, n\}] \\ mB &:= DiagonalMatrix[Table[I \Omega + \mu[i, Bi]^2, \{i, n\}]] \\ mC &:= \frac{I \Omega}{as Bi} * (DiagonalMatrix[Table[\psi[i]'[1], \\ &\hspace{1em} \{i, n\}]] \cdot Table[\psi[i][1], \{j, n\}, \{i, n\}]) \end{aligned}$$

The rules generating the system of ordinary differential equations and the corresponding initial conditions are:

$$\begin{aligned} ode &:= Thread[Table[\theta[i]'[\xi], \{i, n\}] == Inverse[mA] \\ &\hspace{1em} \cdot (mC - mB) \cdot Table[\theta[i][\xi], \{i, n\}]] \\ ic &:= Table[\theta[i][0] == (-2 Bi \theta_2 \psi[i][1] + \mu[i, Bi]^2 \\ &\hspace{1em} ((Bi \theta_0 + 2 \theta_2 + Bi \theta_2) \psi[i][1] + \theta_1 (-\psi[i][0] + \psi[i][1] \\ &\hspace{1em} + Bi \psi[i][1]))) / \mu[i, Bi]^4, \{i, 1, n\}] \end{aligned}$$

The unknown integral transforms are:

```
var := Table[θ[i], {i, n}]
```

Example

First we have to assign values to the global parameters:

```
Bi = 10; Ω = 1.0; as = 8.5 10-3;
θ0 = 1; θ1 = 0; θ2 = -1; n = 25
```

where we have employed a truncation order of 25 terms. The ode problem is:

```
problem = Join[ode, ic]
```

The numerical solution in the axial range $0 < \xi < 5$ for the integral transforms are:

```
sol = First[NDSolve[problem, var, {ξ, 0, 5}]]
```

Introducing these results into the inversion formula we obtain:

$$\theta[\xi, \eta] = \text{Sum}[\psi[i][\eta] \theta[i][\xi], \{i, 1, n\}] /. \text{sol}$$

The temperature, the amplitude and the phase angle at $\xi = 0.5$ and $\eta = 1$ are:

```
{θ[0.5, 1], Abs[θ[0.5, 1]], Arg[0.5, 1]}
{-0.001673 - 0.00505492 I, 0.00532458, -1.89041}
```

The amplitude of the temperature oscillations $\text{Abs}[\theta[\xi, \eta]]$ in $0 \leq \xi \leq \xi_1$ and $0 \leq \eta \leq 1$ are easily plotted by using the *Mathematica* function `Plot3D`. This plot may also include information for a phase angle by using a color scheme [1, p. 139], 2, p. 226].

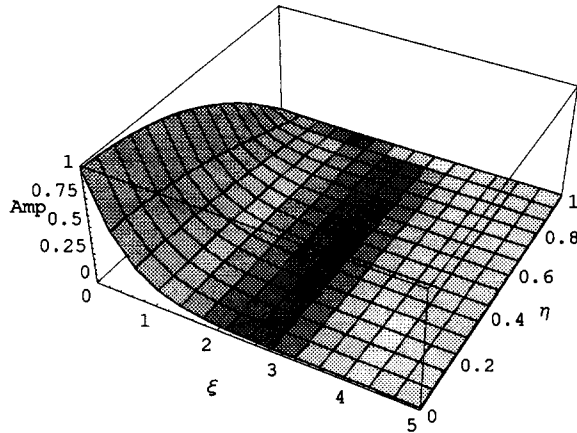


We define the rules:

```
Amplitude[z_Complex] := Abs[z]
Phase[z_Complex] := Hue[N[Arg[z]] / (2 π)]
```

Next, the solution of the above problem is plotted :

```
Plot3D[{Amplitude[θ[ξ, η]], Phase[θ[ξ, η]]}, {ξ, 0, 5}, {η, 0, 1},
AxesLabel → {"ξ", "η", "Amp"}, PlotRange → All];
```



The color plots are printed on shades of gray within the paper. On your monitor you will see colors that appear as the angle moves around the circle. The vertical distances to the surface represent the amplitudes. The phase angle is represented by the color of the surface. Therefore this plot gives all information about the temperature oscillations.

REFERENCES

[1] Gray T.W., Glynn J., *Exploring Mathematics with Mathematica*, Addison-Wesley, 1991.
 [2] Maeder R., *Programming in Mathematica*, Addison-Wesley, 2nd Ed., 1991.